nature materials

ARTICLES

PUBLISHED ONLINE: 17 NOVEMBER 2013 | DOI: 10.1038/NMAT3807

Efficient charge generation by relaxed charge-transfer states at organic interfaces

Koen Vandewal[1]*, Steve Albrecht[2], Eric T. Hoke[1], Kenneth R. Graham[1,3], Johannes Widmer[4], Jessica D. Douglas[5], Marcel Schubert[2], William R. Mateker[1], Jason T. Bloking[1], George F. Burkhard[1], Alan Sellinger[1†], Jean M. J. Fréchet[3,5], Aram Amassian[3], Moritz K. Riede[4†], Michael D. McGehee[1], Dieter Neher[2]* and Alberto Salleo[1]*

Interfaces between organic electron-donating (D) and electron-accepting (A) materials have the ability to generate charge carriers on illumination. Efficient organic solar cells require a high yield for this process, combined with a minimum of energy losses. Here, we investigate the role of the lowest energy emissive interfacial charge-transfer state (CT_1) in the charge generation process. We measure the quantum yield and the electric field dependence of charge generation on excitation of the charge-transfer (CT) state manifold via weakly allowed, low-energy optical transitions. For a wide range of photovoltaic devices based on polymer:fullerene, small-molecule:C_{60} and polymer:polymer blends, our study reveals that the internal quantum efficiency (IQE) is essentially independent of whether or not D, A or CT states with an energy higher than that of CT_1 are excited. The best materials systems show an IQE higher than 90% without the need for excess electronic or vibrational energy.

The mechanism of free charge carrier generation in synthetic organic semiconductors has generated substantial interest recently, as these materials show great promise for low-cost and large-area photovoltaics. In these materials, the lowest energy excited states are strongly bound excitons, which decay before dissociating into free charge carriers with appreciable yield. This fundamental hurdle has been overcome with the introduction of electron-donor/electron-acceptor (D/A) interfaces[1–3]. As opposed to devices consisting of neat organic semiconductors[4,5], free carriers are generated at such interfaces with a yield quasi-independent of photon energy within the spectral range of strong active layer absorption[6–11]. For the best performing materials systems, IQEs approaching and even exceeding 90% (refs 7–11) have been reached. However, free charge carrier generation at organic interfaces is typically associated with an energy loss, which ultimately reduces the power conversion efficiency of the system. Hence, a detailed understanding of the free charge carrier generation mechanisms at organic/organic interfaces, and the origin of the associated energy losses is of crucial importance for future rational design of D and A materials and interfaces.

Figure 1a shows schematically the possible pathways for the generation of free charge carriers on photoexcitation of the donor semiconductor into its excited manifold (D*; ref. 12). At the D/A interface, electron transfer from D* to A results in the formation of a CT state. This CT state can decay to the ground state (GS) or produce the desired charge-separated state (CS), which, unlike the CT state, is not coupled to the GS. In the CS state, the charge carriers have overcome the Coulomb binding energy and can freely migrate in the active layer. Optical transitions between the GS and CT state manifold are however possible and both CT absorption and CT emission at energies below the optical gap of D and A have been detected, albeit with low oscillator strength[13–15].

It has been proposed[16–18] that excess photon energy assists in the generation of free charge carriers. Delocalized, higher energy CT states, dissociating with a rate constant k_{CS}^{*}, are postulated in this case to be the main precursors of free charge carriers. According to this scenario the relaxed emissive CT state (CT_1) will act as a trap and the quantum yield for free carrier generation of this state is expected to be very low and strongly field dependent. If, however, relaxation within the CT state manifold to CT_1 is much faster than charge separation via these higher energy states ($k_{relax} \gg k_{CS}^{*}$), the free carrier yield will be exclusively determined by the competition between dissociation (rate constant k_{CS}) and recombination (rate constant k_f) of the thermally relaxed CT manifold. If free carrier generation follows this mechanism, its quantum yield and field dependence will not depend on photon energy, even for direct excitation into the CT state manifold. Rather, free charge carrier generation will be determined by the interfacial energy landscape, which connects the relaxed CT to the CS states.

By using femtosecond laser spectroscopy it was recently shown that photoexcitation dynamics depend on photon energy. Furthermore, transient absorption signals have been detected on timescales faster than relaxation within the CT manifold[17,18]. These measurements are suggestive of ultrafast CT splitting processes and invoke the role of 'hot' states, where excess energy provided by the energy level offsets between the neat materials is used to overcome the binding energy of interfacial CT states. However, the question

[1]Department of Materials Science and Engineering, Stanford University, 476 Lomita Mall, Stanford, California 94305, USA, [2]Institute of Physics and Astronomy, University of Potsdam, Karl-Liebknecht-Straße 24-25, 14476 Potsdam, Germany, [3]King Abdullah University of Science and Technology (KAUST), Thuwal 23955-6900, Saudi Arabia, [4]Institut für Angewandte Photophysik TU Dresden, George-Bähr-Strasse 1, 01062, Dresden, Germany, [5]Department of Chemistry, University of California, 727 Latimer Hall, Berkeley, California 94720, USA. †Present addresses: Department of Chemistry and Geochemistry, Colorado School of Mines, Golden, Colorado 80401, USA (A.S.); Department of Physics, University of Oxford, Clarendon Laboratory, Parks Road, Oxford OX1 3PU, UK (M.K.R.). *e-mail: vandewal@stanford.edu; neher@uni-potsdam.de; asalleo@stanford.edu

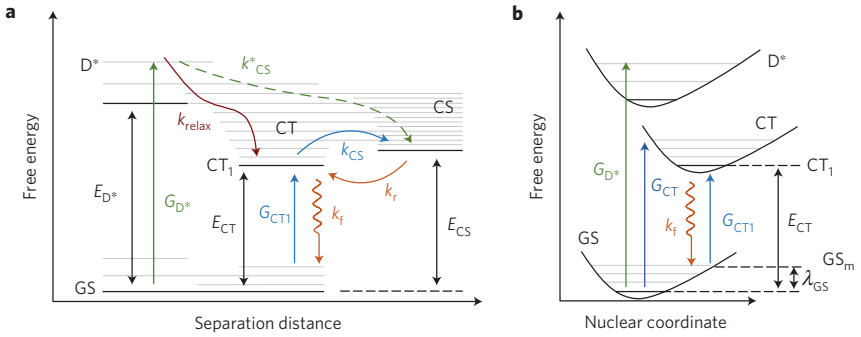

Figure 1 | Energetics of the relevant states at a D/A interface. a, State diagram. Absorption of a photon with energy higher than E_{D*} generates the donor excited state D* at a rate G_{D*}. There are several possible pathways for the generation of a CS state. Pathways with rate constants k^*_{CS} bypass the vibrationally relaxed and lowest energy CT state (CT_1) and compete with thermal relaxation (k_{relax}). CT_1 can decay radiatively (k_f) to the GS or dissociate (k_{CS}), forming CS. The inverse of the latter process, population of CT_1 from CS, occurs at a rate k_r. **b**, Potential energy surfaces of GS, and low-energy CT and D* states. Higher energy electronic CT and D* states are omitted for clarity. Optical excitation into CT_1 (G_{CT1}) occurs on excitation with a photon energy $E_{CT} - \lambda_{GS}$, from the vibrationally excited ground state GS_m. Such transitions from higher energy ground states are the inverse of CT emission, which peaks at photon energy $E_{CT} - \lambda_{GS}$.

remains as to the extent by which these 'hot' effects influence the actual photovoltaic device performance. Further, it is unclear whether CT_1 is always necessarily strongly bound ($E_{CS} - E_{CT} \gg kT$, where k is the Boltzmann constant and T the temperature) or whether there exists the possibility in some D/A systems that CT_1 is sufficiently delocalized to ensure efficient dissociation of this state.

This work aims at determining whether charge separation at D/A heterojunctions illuminated by sunlight is mainly preceded by the formation of a thermally relaxed CT state (CT_1) or whether it predominantly occurs via higher energy, more delocalized CT states, bypassing CT_1. To elucidate to what extent the 'hot' CT states play a role in the charge carrier generation mechanism, a determination of the quantum yield and field dependence of charge generation as a function of excitation energy, down to selective excitation of CT_1, is necessary.

Here, we present measurements of the field dependence of charge carrier generation on direct excitation of the CT state manifold. The presence of such field dependence is taken as a hallmark of the need for a driving force to dissociate CT states into free charge carriers. To investigate whether photon energy in excess of the CT_1 energy can provide this driving force, we perform a detailed analysis of electroluminescence emission spectra and external quantum efficiency (EQE) spectra. Sensitive techniques allow us to determine the quantum yield of carrier generation by CT_1 and compare it with the carrier generation yield for higher energy D, A and CT excitations. We study a number of D/A combinations including polymer:fullerene, small-molecule:C_{60} and polymer:polymer blends with varying photovoltaic performance and, surprisingly, find that the field dependence and absolute value of the quantum yield for free carrier generation for all studied D/A interfaces has little dependence on whether or not the initially generated excited state has energy in excess of the energy of CT_1. Importantly, we demonstrate that a high and field-independent IQE does not necessarily require that free carrier formation proceeds primarily via higher energy 'hot' states. In fact, present state-of-the-art bulk heterojunction layers produce a high yield of free charge carriers (>90%) because of very efficient dissociation of CT_1 into free charge carriers.

First we compare two polymer:$PC_{61}BM$ model systems, which, on excitation of the donor polymer, have respectively a relatively inefficient and field-dependent charge carrier generation mechanism (MEH-PPV:$PC_{61}BM$), and an efficient and field-independent charge carrier generation mechanism (PBDTTPD:$PC_{61}BM$). Figure 2a,b shows current density–voltage (J–V) curves under solar illumination and in the dark of photovoltaic devices prepared with these blends as active layers. The devices have a power conversion efficiency of ~1.3% (MEH-PPV:$PC_{61}BM$) and ~7% (PBDTTPD:$PC_{61}BM$). Device preparation details can be found in the Supplementary Information. The field dependence of the charge carrier generation mechanism on photoexcitation of the D*, A* and CT manifold is investigated by time-delayed collection field (TDCF) experiments. The total extracted charge carrier density using this technique is a direct measure of the free carrier generation yield at a certain bias voltage[19,20]. The relative yield, as a function of bias voltage and excitation energy, is shown on the right axes in Fig. 2a,b, allowing comparison with the photocurrent, that is, the difference between the J–V curves taken in darkness and under illumination. For the MEH-PPV:$PC_{61}BM$ device, the dependence of the photocurrent on voltage tracks the dependence of the charge carrier generation yield on voltage, indicating that its performance is limited by its strongly field-dependent charge carrier generation mechanism, consistent with previous reports on PPV:$PC_{61}BM$ devices[21,22]. In contrast, for the PBDTTPD:$PC_{61}BM$ device, the yield is field independent, and reaches almost unity[11]. On varying the excitation photon energy, we can selectively excite mainly the D* and/or A* and CT state manifold. For the MEH-PPV:$PC_{61}BM$ and PBDTTPD:$PC_{61}BM$ devices, a TDCF signal could still be detected at excitation photon energies as low as 1.38 eV and 1.53 eV, respectively. This energy is well below the optical gap of the neat materials comprising the blend, and charge carrier generation at this photon energy is the result of direct CT state excitation (see also Fig. 3). Importantly, we observe virtually no differences in the field dependence of charge carrier generation. This is valid, irrespective of whether the charge generation mechanism is field dependent (MEH-PPV:$PC_{61}BM$) or field independent (PBDTTPD:$PC_{61}BM$).

This result is consistent with previous work, in which the CT state manifold was directly excited and no differences in charge generation efficiency[23], IQE (ref. 24) and field dependence of EQE (ref. 25) were found when compared with higher energy D* and A* excitation. However, as all of these experiments are limited in sensitivity and spectral range, they do not access the lowest energy CT_1 state exclusively and therefore do not provide a clear answer as to whether the CT_1 state is the exclusive free carrier precursor. Indeed, owing to the significant reorganization of the nuclei following optical excitation, transitions into the CT state manifold will dominantly result in a vibrationally excited CT state (Fig. 1b). No experiment has yet compared quantum

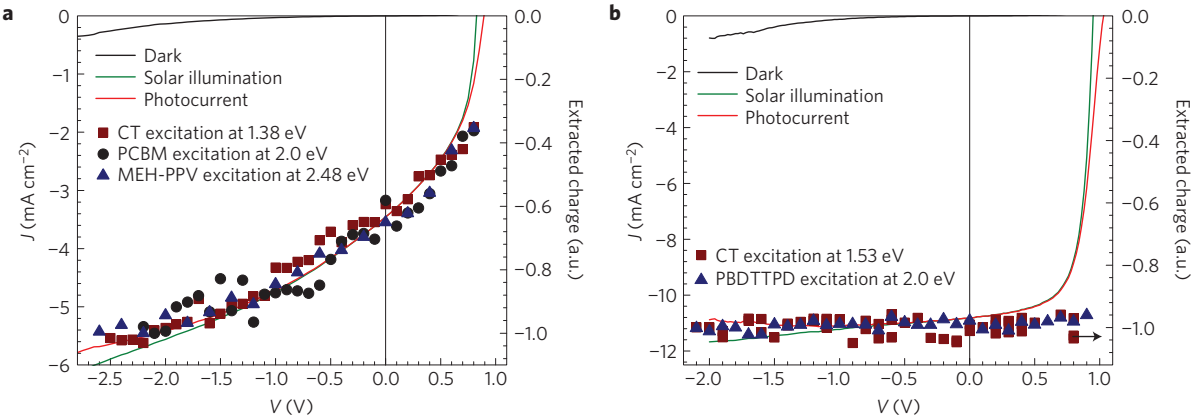

Figure 2 | Current density and relative number of photogenerated charge carriers as a function of applied voltage. a,**b**, *J*–*V* curves in the dark and under solar illumination for a solution-processed MEH-PPV:$PC_{61}BM$ device (**a**) and for a PBDTTPD:$PC_{61}BM$ device (**b**). The relative number of generated charge carriers, extracted in the TDCF experiment as a function of applied bias, is shown on the right axis, for dominant excitations of D*, A* and those directly into the CT band (at 1.38 eV for MEH-PPV:$PC_{61}BM$ and 1.5 eV for PBDTTPD:$PC_{61}BM$).

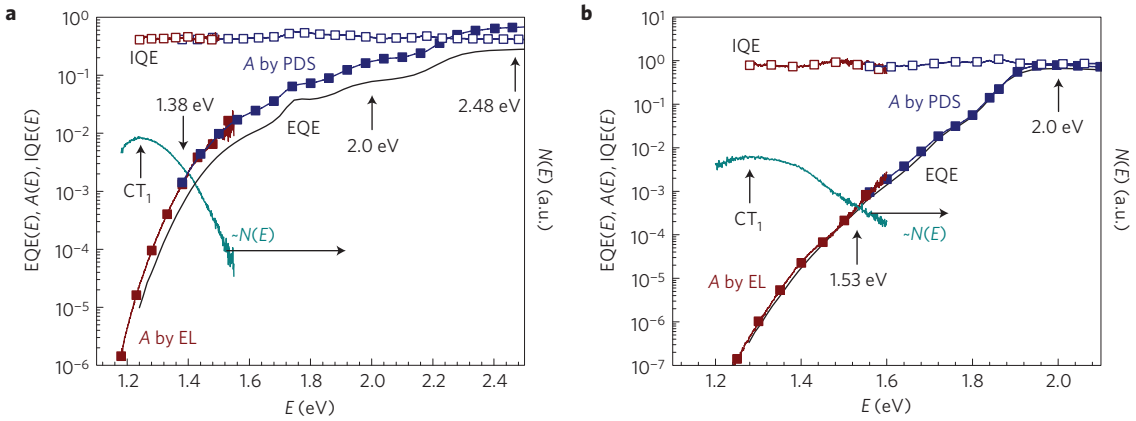

Figure 3 | Determination of IQE(*E*) in the spectral region of CT emission for polymer:fullerene photovoltaic devices. EQE(*E*) (black line), electroluminescence (EL) emission spectra *N*(*E*) (cyan line) and the high energy part of the *A*(*E*) spectra (blue line filled squares) are measured directly on photovoltaic devices and active layers. In the very weakly absorbing region, the *A*(*E*) spectra are reconstructed using *N*(*E*) as described in the main text, and are matched to the *A*(*E*) spectra measured by PDS in the overlapping region (red line, filled squares). **a**,**b**, Data for a solution-processed MEH-PPV:$PC_{61}BM$ device (**a**) and for a PBDTTPD:$PC_{61}BM$ device (**b**). The IQE(*E*) spectra (open squares) of the devices are calculated as EQE(*E*)/*A*(*E*). The arrows indicate the $GS_m \rightarrow CT_1$ transition at 1.24 eV for MEH-PPV:$PC_{61}BM$ and 1.28 eV for PBDTTPD:$PC_{61}BM$. The arrows indicate the excitation energies at which the TDCF experiments shown in Fig. 2 were performed.

yields of free carrier generation of the reorganized, emissive and completely relaxed CT state (CT_1) with that of higher energy CT, D* or A* excitations. This is therefore precisely what we aim to do in this work.

Direct excitation of CT_1 exclusively involves a photon having an energy $E_{CT} - \lambda_{GS}$ (Fig. 1b) exciting an electron from a higher energy level of the GS manifold, GS_m, to CT_1. This transition is severely suppressed as compared with the already weak CT absorption by the low probability of thermal population of GS_m ($\exp(-\lambda_{GS}/kT) = 4 \times 10^{-4}$ for a typical value of $\lambda_{GS} = 0.2$ eV). Hence, the direct measurement of the $GS_m \rightarrow CT_1$ absorption is very challenging. As a result, here we follow another approach and reconstruct the absorption spectrum $A(E)$ in this low-energy region by measuring the inverse optical process, that is, radiative decay from the thermally relaxed CT manifold, which is dominated by the $CT_1 \rightarrow GS_m$ transition at a photon energy $E_{CT} - \lambda_{GS}$. When the population of the excited states, including the vibrational states within the CT state manifold, are in thermal equilibrium during the emission experiment, the fraction of absorbed photons $A(E)$ at any given photon energy E is related to the flux of photons emitted at this energy, $N(E)$, by the following equation[26,27]

$$A(E) \sim N(E)E^{-2}\exp\left(\frac{E}{kT}\right) \quad (1)$$

In the Supplementary Information, we summarize how Boltzmann occupation of the excited- and ground-state energy levels and optical reciprocity lead to equation (1). Equation (1) provides us with a determination of the relative optical absorption strength in the spectral region where CT emission is measurable. A sensitive measurement of the EQE spectrum over the same spectral region will allow us to compare the IQE of CT_1 excitation, which occurs at the photon energy where the CT emission peaks, with the IQE of excitation into higher energy states.

In Fig. 3a,b we reconstruct the absorption spectrum of the MEH-PPV:$PC_{61}BM$ and PBDTTPD:$PC_{61}BM$ devices, for photon energies corresponding to CT_1 excitation and higher. The emission spectra N(E), also shown in Fig. 3a,b, are obtained by electroluminescence

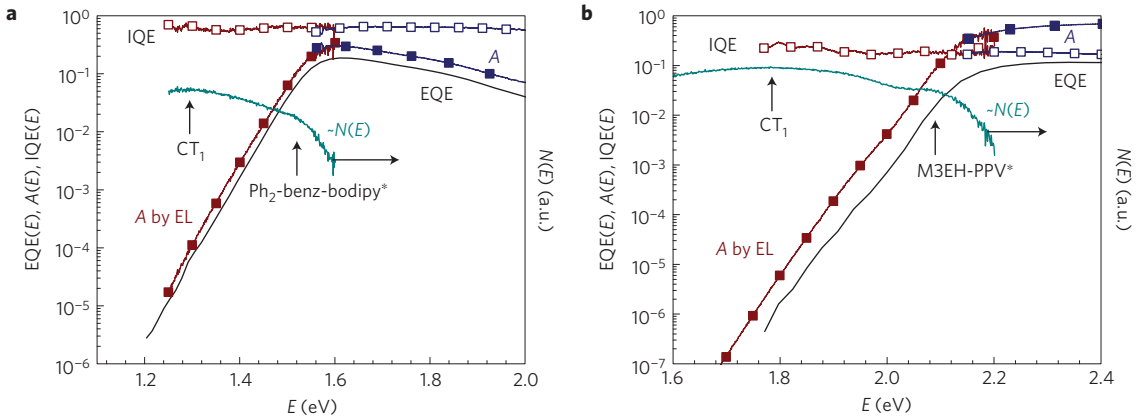

Figure 4 | Determination of IQE(*E*) in the spectral region of CT emission for small-molecule:C_{60} and polymer:polymer photovoltaic devices. EQE(*E*) (black line), electroluminescence (EL) emission spectra *N*(*E*) (cyan line) and *A*(*E*) spectra (blue line filled squares) are measured directly on photovoltaic devices. *A*(*E*) spectra are reconstructed using *N*(*E*) as described in the main text and are matched to the *A*(*E*) spectra measured with the aid of an integrating sphere in the strongly absorbing spectral region (red line, filled squares). **a**,**b**, Data for a vacuum processed Ph_2-benz-bodipy:C_{60} small-molecule device (**a**) and for a M3EH-PPV:CN-ether-PPV polymer:polymer device (**b**). The IQE(*E*) spectra (open squares) of the devices are calculated as EQE(*E*)/*A*(*E*). The arrows indicate the $GS_m \rightarrow CT_1$ transition at 1.30 eV for Ph_2-benz-bodipy:C_{60} and 1.78 eV for M3EH-PPV:CN-ether-PPV. Radiative decay from donor excitations is still observable in the emission spectrum at 1.55 eV and 2.07 eV, respectively.

measurements using an as low as possible injection current $<30\,mA\,cm^{-2}$, to ensure quasi-equilibrium conditions. Indeed, the spectral shape is independent of the injection current in the low injection current regime (see Supplementary Information). In the measurable energy range, electroluminescence spectra consist of CT emission alone. The >10 ns lifetime of the injected free charge carriers in the devices during the electroluminescence experiment makes it nearly certain that thermal equilibrium within the CT state manifold is reached before radiative decay to the GS, thereby obeying Kasha's rule[28]. Under this condition, we can use equation (1) to calculate the spectral shape of *A*(*E*) in the region of CT emission. The absorption spectrum at higher energies is still weak, but sufficiently high to be detectable by the sensitive photothermal deflection spectroscopy (PDS). Matching the spectra in the overlapping region allows us to set *A*(*E*) determined by electroluminescence experiments to an absolute scale. In the MEH-PPV:PC_{61}BM case, we use the overlapping region to determine the temperature (*T*) of the active layer during the emission experiments, using equation (1), to be 35 °C, slightly above room temperature, as expected[29]. For all devices studied in this work, we use similar injection currents and assume $T = 35\,°C$. Details about possible uncertainties introduced by the uncertainty on the temperature of the active layer during the emission experiment can be found in the Supplementary Information.

The EQE(*E*) spectrum of both photovoltaic devices is measured by a sensitive lock-in technique. The IQE(*E*), calculated as EQE(*E*)/*A*(*E*), is shown together with the EQE(*E*) in Fig. 3a,b. Note that the use of a sensitive EQE(*E*) measurement set-up allows us to detect a photocurrent signal even at very low photon energies corresponding to the peak of CT emission, that is, the optical transition between GS_m and CT_1 (Fig. 1b). Within the sensitivity of the method, the IQE for this transition is essentially identical to the IQE at higher energies including D* or A* excitation. This observation is valid for the MEH-PPV:PC_{61}BM active layer, which has a field-dependent charge generation yield as well as for the PBDTTPD:PC_{61}BM active layer, which has a field-independent IQE of about 90% (ref. 11). If the yield for free charge carrier generation via CT_1 were strongly suppressed as compared with the higher energy states, one would expect a strongly decreasing IQE(*E*) near the photon energy at which CT emission peaks, contrary to our observations.

To investigate the generality of this result for other types of D/A interface, we study devices made with a vacuum-processed small-molecule Ph_2-benz-bodipy:C_{60} blend[30,31], as well as a M3EH-PPV:CN-ether-PPV (ref. 32) polymer:polymer blend as the active layer. For both materials systems, the CT state energy is close to the optical gap of the donor. Therefore, population of D* during the electroluminescence experiment becomes probable, and the electroluminescence spectra of these devices, shown in Fig. 4, contain a band related to emission from excited donor (at 1.55 eV and 2.07 eV, for the small-molecule and polymer:polymer device respectively) in addition to the CT emission band (centred at 1.30 eV and 1.78 eV, respectively). As a result we are able to reconstruct *A*(*E*) using the electroluminescence emission spectrum and equation (1), up to photon energies where the donor material is strongly absorbing. A measurement of *A*(*E*) in the strongly absorbing region by conventional integrating sphere ultraviolet–visible spectroscopy is used to set *A*(*E*) to absolute scale, down to excitation into CT_1. For both the vacuum-processed and polymer:polymer blend devices, IQE(*E*) does not vary significantly within the energy range from CT_1 up to donor excitation.

To broaden the validity of our result, we studied eight additional organic photovoltaic devices based on D:A blends with varying performances and IQEs and found comparable results (see Supplementary Information). The IQE(*E*) remains virtually constant for excitation energies ranging from the CT emission peak—and in some cases even for excitation energies lower than the emission peak (Supplementary Figs 7–9)—to the CT absorption peak. These measurements indicate that, for the studied D:A blends, energy in excess of the CT_1 energy, including reorganization energy within the CT manifold, does not affect the IQE. Free charge carriers are generated and collected with equal efficiency by excitation directly into CT_1, as by excitation into higher energy, unrelaxed CT states or even D* or A* states.

Even though femtosecond transient spectroscopy has shown the existence of higher energy, faster dissociating pathways at these organic/organic interfaces[17,18,33], our results indicate that population and subsequent dissociation of these higher energy CT states directly following photoinduced electron transfer is not responsible for most of the generated free charge carriers. We propose that, owing to ultrafast relaxation within the CT band, most photoexcitations into higher energy states relax within the

CT manifold and are in thermal equilibrium with CT_1. As a consequence, for D/A interfaces at which CT_1 is a bound state, the overall IQE at all photon energies, down to exclusive CT_1 excitation, will be significantly lower than unity, and electric field dependent (for example, MEH-PPV:$PC_{61}BM$, M3EH-PPV:CN-ether-PPV). The general validity of our result across materials systems and cell efficiencies suggests that excess energy provided by D*, A* or higher energy CT excitation cannot by exploited to improve the free carrier yield. However, the remarkably high (>90%) and field-independent yield of free charge carrier generation via CT_1 in the PBDTTPD:$PC_{61}BM$ and PCDTBT:$PC_{71}BM$ (see Supplementary Information) devices shows that materials systems exist, in which CT_1 is only weakly bound, yielding efficient >90% charge generation at all photon energies equal to and larger than the energy of CT_1. Therefore, understanding and control over the nanostructural factors that allow an interfacial energy landscape in which CT_1 is sufficiently delocalized, with an energy close to the energy of the CS state, is of fundamental importance for designing and developing new, better performing D/A pairs for organic photovoltaics.

Methods

Photovoltaic devices comprising polymer:fullerene and polymer:polymer active layers were prepared in the standard device configuration ITO/PEDOT:PSS (40 nm)/active layer/(7 nm) Ca/(200 nm) Al, using their optimized D/A ratio and solution concentration (more details specific to the materials system used can be found in the Supplementary Information). Small-molecule:C_{60} bulk heterojunction devices were vacuum deposited in the configuration ITO/hole conductor/active layer/electron conductor/Al. Specific details such as D/A stoichiometry and used electron on hole transporting layers can be found in the Supplementary Information.

TDCF experiments use a pulsed excitation (5.5 ns pulse duration, 500 Hz repetition rate) with a diode-pumped, Q-switched Nd:YAG laser (NT242,EKSPLA) frequency tripled to pump an optical parametric oscillator for wavelength tuning. The current through the photovoltaic device was measured using a 50 Ω resistor placed in series and was recorded with a Yokogawa DL9140 oscilloscope. An Agilent 81150A pulse generator with a very fast slew rate was used to apply the pre- and collection bias to the sample. Note that we can rule out any residual parasitic wavelengths (that is, 1,064, 512 or 355 nm or the optical parametric oscillator idler if signal was used) by carefully checking the beam quality at the position of the sample with a spectrophotometer. The collection bias was kept low at ∼−3 V. This ensures that the leakage during extraction is small and at the same time the loss due to non-geminate recombination during extraction is prevented for the studied systems.

Electroluminescence spectra were measured using a spectrograph (Acton Research SpectraPro 500i) equipped with a silicon CCD (charge-coupled device) array detector (Hamamatsu), and were corrected for the instrument response and the conversion from wavelength to energy.

Sensitive EQE measurements were taken at short circuit under focused monochromated illumination from a 100 W tungsten lamp modulated by an optical chopper (∼280 Hz). The current from the devices was measured as a function of photon energy using a lock-in amplifier (Stanford Instruments SR 830) and compared with the current obtained from a calibrated Ge or Si photodiode.

PDS was performed using a home-built set-up: chopped (3.333 Hz) monochromated light from a 150 W Xe lamp is focused onto the sample. Perfluorohexane (C_6F_{14}, 3M Fluorinert FC-72) is used as the deflection medium. The deflection of a HeNe laser (633 nm) is detected by a position-sensitive Si detector, connected to a Stanford Research Systems SR830 lock-in amplifier. PDS samples of active layers were spin-coated on quartz substrates, from the same solution from which the devices were fabricated. The PDS spectra were set to absolute scale by matching the spectra with integrating sphere measurements on a Varian Cary 5000 spectrophotometer. $A(E)$ in the weakly absorbing subgap region was calculated by the simplified assumption of the incoming light waves passing through the active layer twice owing to reflection from the metallic cathode.

Received 22 May 2013; accepted 8 October 2013; published online 17 November 2013

References

1. Deibel, C. & Dyakonov, V. Polymer–fullerene bulk heterojunction solar cells. *Rep. Prog. Phys.* **73,** 096401 (2010).
2. Riede, M., Mueller, T., Tress, W., Schueppel, R. & Leo, K. Small-molecule solar cells—status and perspectives. *Nanotechnology* **19,** 424001 (2008).
3. Li, G., Zhu, R. & Yang, Y. Polymer solar cells. *Nature Photon.* **6,** 153–161 (2012).
4. Arkhipov, V. I., Emelianova, E. V. & Bässler, H. Hot exciton dissociation in a conjugated polymer. *Phys. Rev. Lett.* **82,** 1321–1324 (1999).
5. Tong, M., Coates, N. E., Moses, D., Heeger, A. J., Beaupré, S. & Leclerc, M. Charge carrier photogeneration and decay dynamics in the poly (2, 7-carbazole) copolymer PCDTBT and in bulk heterojunction composites with $PC_{70}BM$. *Phys. Rev. B* **81,** 125210 (2010).
6. Vandewal, K. *et al.* Quantification of quantum efficiency and energy losses in low bandgap polymer: Fullerene solar cells with high open-circuit voltage. *Adv. Funct. Mater.* **22,** 3480–3490 (2012).
7. Hou, J., Chen, H.-Y., Zhang, S., Chen, R. I., Yang, Y., Wu, Y. & Li, G. Synthesis of a low band gap polymer and its application in highly efficient polymer solar cells. *J. Am. Chem. Soc.* **131,** 15586 (2009).
8. Liang, Y. *et al.* For the bright future-bulk heterojunction polymer solar cells with power conversion efficiency of 7.4%. *Adv. Mater.* **22,** E135–E138 (2010).
9. Park, S. H. *et al.* Bulk heterojunction solar cells with internal quantum efficiency approaching 100%. *Nature Photon.* **3,** 297–302 (2009).
10. Lin, L-Y. *et al.* A donor–acceptor–acceptor molecule for vacuum-processed organic solar cells with a power conversion efficiency of 6.4%. *Chem. Commun.* **48,** 1857–1859 (2012).
11. Bartelt, J. A. *et al.* The importance of fullerene percolation in the mixed regions of polymer–fullerene bulk heterojunction solar cells. *Adv. Energy Mater.* **3,** 364–374 (2013).
12. Brédas, J. L., Norton, J. E., Cornil, J. & Coropceanu, V. Molecular understanding of organic solar cells: The challenges. *Acc. Chem. Res.* **42,** 1691–1699 (2009).
13. Benson-Smith, J. J. *et al.* Formation of a ground-state charge-transfer complex in polyfluorene/[6, 6]-phenyl-c61 butyric acid methyl ester (PCBM) blend films and its role in the function of polymer/PCBM solar cells. *Adv. Funct. Mater.* **17,** 451–457 (2007).
14. Loi, M. A. *et al.* Charge transfer excitons in bulk heterojunctions of a polyfluorene copolymer and a fullerene derivative. *Adv. Funct. Mater.* **17,** 2111–2116 (2007).
15. Vandewal, K., Tvingstedt, K., Gadisa, A., Inganäs, O. & Manca, J. V. On the origin of the open-circuit voltage of polymer–fullerene solar cells. *Nature Mater.* **8,** 904–909 (2009).
16. Ohkita, H. *et al.* Charge carrier formation in polythiophene/fullerene blend films studied by transient absorption spectroscopy. *J. Am. Chem. Soc.* **130,** 3030–3042 (2008).
17. Bakulin, A. A. *et al.* The role of driving energy and delocalized states for charge separation in organic semiconductors. *Science* **335,** 1340–1344 (2012).
18. Grancini, G. *et al.* Hot exciton dissociation in polymer solar cells. *Nature Mater.* **12,** 29–33 (2013).
19. Kniepert, J., Schubert, M., Blakesley, J. C. & Neher, D. Photogeneration and recombination in P3HT/PCBM solar cells probed by time-delayed collection field experiments. *J. Phys. Chem. Lett.* **2,** 700–705 (2011).
20. Albrecht, S. *et al.* On the field dependence of free charge carrier generation and recombination in blends of PCPDTBT/PC70BM: Influence of solvent additives. *J. Phys. Chem. Lett.* **3,** 640–645 (2012).
21. Mihailetchi, V. D., Koster, L. J. A., Hummelen, J. C. & Blom, P. W. M. Photocurrent generation in polymer–fullerene bulk heterojunctions. *Phys. Rev. Lett.* **93,** 216601 (2004).
22. Mingebach, M., Walter, S., Dyakonov, V. & Deibel, C. Direct and charge transfer state mediated photogeneration in polymer–fullerene bulk heterojunction solar cells. *Appl. Phys. Lett.* **100,** 193302 (2012).
23. Parkinson, P., Lloyd-Hughes, J., Johnston, M. B. & Herz, L. M. Efficient generation of charges via below-gap photoexcitation of polymer–fullerene blend films investigated by terahertz spectroscopy. *Phys. Rev. B* **78,** 115321 (2008).
24. Lee, J. *et al.* Charge transfer state versus hot exciton dissociation in polymer–fullerene blended solar cells. *J. Am. Chem. Soc.* **132,** 11878–11880 (2010).
25. Van der Hofstad, T. G. J., Di Nuzzo, D., van den Berg, M., Janssen, R. A. J. & Meskers, S. C. J. Influence of photon excess energy on charge carrier dynamics in a polymer–fullerene solar cell. *Adv. Energy Mater.* **2,** 1095–1099 (2012).
26. Würfel, P. The chemical potential of radiation. *J. Phys. C* **15,** 3967–3985 (1982).
27. Würfel, P. *The Physics of Solar Cells* (Wiley, 2007).
28. Kasha, M. Characterization of electronic transitions in complex molecules. *Discuss. Faraday Soc.* **9,** 14–19 (1950).
29. Lupton, J. M. Frequency up-conversion as a temperature probe of organic opto-electronic devices. *Appl. Phys. Lett.* **80,** 186–188 (2002).
30. Gresser, R., Hummert, M., Hartmann, H., Leo, K. & Riede, M. Synthesis and characterization of near-infrared absorbing benzannulated Aza-BODIPY dyes. *Chem. Eur. J.* **17,** 2939–2947 (2011).
31. Meiss, J., Holzmueller, F., Gresser, R., Leo, K. & Riede, M. Near-infrared absorbing semitransparent organic solar cells. *Appl. Phys. Lett.* **99,** 193307 (2011).

32. Yin, C. *et al.* Tuning of the excited-state properties and photovoltaic performance in PPV-based polymer blends. *J. Phys. Chem. C* **112,** 14607–14617 (2008).
33. Jailaubekov, A. E. *et al.* Hot charge-transfer excitons set the time limit for charge separation at donor/acceptor interfaces in organic photovoltaics. *Nature Mater.* **12,** 66–73 (2013).

Acknowledgements

This publication was supported by the Center for Advanced Molecular Photovoltaics (Award No KUS-C1-015-21) and the Department of Energy, Laboratory Directed Research and Development funding, under contract DE-AC02-76SF00515. The PCDTBT used in this work was provided by St-Jean Photochemicals. M.K.R. acknowledges financial support by the BMBF through project 03IP602 and J.W. acknowledges support from the Heinrich-Böll-Stiftung. S.A. and M.S. acknowledge financial support by the BMBF within PVcomB (FKZ 03IS2151D) and the DFG (SPP 1355). D.N. thanks the DFG for financially supporting a travel grant. K.R.G. and A.A. acknowledge SABIC for a post-doctoral fellowship. The authors thank J. Kurpiers for technical assistance with the TDCF set-up.

Author contributions

K.V., D.N., S.A. and A. Salleo designed the experiments. S.A. prepared devices for TDCF experiments and performed the TDCF experiments. K.V., W.R.M., E.T.H., K.R.G., J.T.B., M.S., J.W. and M.K.R. prepared photovoltaic devices and optimized their processing parameters for photovoltaic performance. E.T.H. and J.T.B. adjusted the EQE and electroluminescence measurement set-ups for the detection of weak signals, crucial for this work. K.V., E.T.H. and K.R.G. measured the EQE and electroluminescence spectra. K.V. measured the PDS spectra. J.D.D. synthesized PBDTTPD. A. Sellinger, J.M.J.F., A.A., M.K.R. and M.D.M. supervised their team members involved in the project. D.N. and A. Salleo supervised the overall project. All authors contributed to analysis and writing.

Additional information

Supplementary information is available in the online version of the paper. Reprints and permissions information is available online at www.nature.com/reprints. Correspondence and requests for materials should be addressed to K.V., D.N. or A.S.

Competing financial interests

The authors declare no competing financial interests.